Skin anti-photoaging properties of ginsenoside Rh2 epimers in UV-B-irradiated human keratinocyte cells

SUN-JOO OH[1,†], SIHYEONG LEE[2,†], WOO-YONG CHOI[2] and CHANG-JIN LIM[2,*]

[1]*Department of Biological Sciences and* [2]*Department of Biochemistry, Kangwon National University, Chuncheon 200-701, Korea*

**Corresponding author (Fax, +82-33-259-5664; Email, cjlim@kangwon.ac.kr)*

[†]*These authors contributed equally to this work.*

Ginseng, one of the most widely used herbal medicines, has a wide range of therapeutic and pharmacological applications. Ginsenosides are the major bioactive ingredients of ginseng, which are responsible for various pharmacological activities of ginseng. Ginsenoside Rh2, known as an antitumour ginsenoside, exists as two different stereoisomeric forms, 20(*S*)-ginsenoside Rh2 [20(*S*)-Rh2] and 20(*R*)-ginsenoside Rh2 [20(*R*)-Rh2]. This work aimed to assess and compare skin anti-photoaging activities of 20(*S*)-Rh2 and 20(*R*)-Rh2 in UV-B-irradiated HaCat cells. 20(*S*)-Rh2, but not 20(*R*)-Rh2, was able to suppress UV-B-induced ROS production in HaCat cells. Both stereoisomeric forms could not modulate cellular survival and NO level in UV-B-irradiated HaCat cells. Both 20(*S*)-Rh2 and 20(*R*)-Rh2 exhibited suppressive effects on UV-B-induced MMP-2 activity and expression in HaCat cells. In brief, the two stereoisomers of ginsenoside Rh2, 20(*S*)-Rh2 and 20(*R*)-Rh2, possess skin anti-photoaging effects but possibly in different fashions.

[Oh S-J, Lee S, Choi W-Y and Lim C-J 2014 Skin anti-photoaging properties of ginsenoside Rh2 epimers in UV-B-irradiated human keratinocyte cells. *J. Biosci.* **39** 673–682] **DOI** 10.1007/s12038-014-9460-x

1. Introduction

Among solar ultraviolet (UV) radiation, such as UV-A (315–400 nm), UV-B (280–315 nm) and UV-C (200–280 nm), UV-B, particularly damaging to the basal cell layer of the epidermis, induces skin changes such as wrinkle formation, epidermal thickening, degradation of matrix macromolecules, vascularization and immunosuppression (Barresi *et al.* 2011; Birch-Machin and Swalwell 2010). UV-B-induced skin damages can be either direct due to UV-B absorption by target biomolecules, or indirect in response to the generation of ROS. UV-B causes the immediate generation of superoxide radical in keratinocytes, which is subsequently converted to other ROS species, such as hydrogen peroxide and hydroxyl radical (Aitken *et al.* 2007). UV-B is harmful to epidermal keratinocytes via the induction of inflammatory cytokines, chemokines and prostaglandins, which is responsible for cutaneous reactions such as inflammation, hyperpigmentation, erythema, hyperproliferation and carcinogenesis (Ichihashi *et al.* 2003).

MMPs are implicated in remodeling extracellular matrix structures in wound healing, skin photoaging, and severe pathologies such as carcinogenesis (Curran and Murray 1999; Kähäri and Saarialho-Kere 1997; Werb 1997). MMP-1 (interstitial collagenase), produced by both dermal fibroblasts and epidermal keratinocytes, cleaves type I and III collagen into specific fragments, and these fragments are further degraded by other MMPs, including MMP-2 (gelatinase A) and MMP-9 (gelatinase B). Destruction of collagen, a direct cause of skin aging in both naturally aged

Keywords. Anti-photoaging; ginsenoside Rh2; matrix metalloproteinase; *Panax ginseng* C.A. Meyer; reactive oxygen species

Abbreviations used: MMP, matrix metalloproteinase; NO, nitric oxide; 20(*R*)-Rh2, 20(*R*)-ginsenoside Rh2; 20(*S*)-Rh2, 20(*S*)-ginsenoside Rh2; ROS, reactive oxygen species

Published online: 16 July 2014

and photoaged skins, is linked with the induction of MMPs, which are secreted by epidermal keratinocytes and dermal fibroblasts (Lee *et al.* 2009).

Ginseng, the root of *Panax ginseng* C.A. Meyer (family Araliaceae), is used as a general tonic to promote human health in traditional medicine all over the world. Ginsenosides are responsible for the majority of pharmacological efficacies of ginseng (Baek *et al.* 1996). They are categorized into the three types based on aglycone moieties: protopanaxadiol (PPD)-type ginsenosides (Ra1, Ra2, Ra3, Rb1, Rb2, Rb3, Rc, Rd, Rg3, Rh2, etc.), protopanaxatriol (PPT)-type ginsenosides (Re, Rg1, Rg2, Rf, Rh1, etc.), and oleanolic acid-type ginsenosides (Ro, etc). Rh2, originally identified as an antitumour PPD-type ginsenoside, possesses other pharmacological properties, such as anti-diabetic, anti-obesitic, memory-enhancing, antiallergic, and anti-inflammatory activities (Park *et al.* 2003; Hwang *et al.* 2007). Although native ginseng contains minute amounts of Rh2, some PPD-type ginsenosides, such as Rg3, Rb1, Rb2 and Rc, are metabolized to Rh2 by human intestinal bacteria (Bae *et al.* 2004). Rh2 can be enriched by *in vitro* fermentation using lactic acid bacteria, such as *Bifidobacterium* sp. and *Lactobacillus* sp. (Trinh *et al.* 2007).

Rh2 exists in two stereoisomeric forms, 20(*R*)-Rh2 and 20(*S*)-Rh2, based on a chiral center at C-20 in its molecular structure (figure 1). In recent years, purified Rh2 stereoisomers have been separately used to understand their stereospecific characteristics and structure-function relationship. 20(*R*)-Rh2 only selectively exhibits an inhibitory activity on osteoclastgenesis without any cytotoxicity up to 100 μM in the preosteoclastic cell line RAW264 cells (Liu *et al.* 2009). Compared to 20(*R*)-Rh2, 20(*S*)-Rh2 displays a significant anticancer activity through blocking cell proliferation and causing G1 arrest in human lung adenocarcinoma cells (Zhang *et al.* 2011). Similarly, 20(*S*)-Rh2, but not 20(*R*)-Rh2, suppresses proliferation of androgen-dependent and androgen-independent prostate cancer cells (Liu *et al.* 2010). These findings imply that the stereochemistry of the hydroxyl group at C-20 plays a crucial role in antitumour activity of Rh2. 20(*S*)-Rh2 enhances the oral absorption of digoxin, a classic permeability-glycoprotein substrate, in a dose-dependent manner in rats, whereas 20(*R*)-Rh2 at low dosages increases the oral absorption of digoxin, but this enhancing effect is diminished with its elevated dosages (Zhang *et al.* 2012). This finding suggests that both 20(*S*)-Rh2 and 20(*R*)-Rh2 act as permeability-glycoprotein inhibitors but in a different fashion.

In the process of developing ginsenoside-containing anti-aging cosmetics, we are trying to search for effective ginsenoside(s) which can play a protective role against skin photoaging due to UV radiation. Suppression of ROS level and MMP inhibitory activity became our primary focuses for evaluating skin anti-photoaging properties of 20(*S*)-Rh2 and 20(*R*)-Rh2. In this work, anti-photoaging activities of the two Rh2 stereoisomers, 20(*S*)-Rh2 and 20(*R*)-Rh2, were examined and compared in UV-B-irradiated human keratinocyte HaCat cells.

2. Materials and methods

2.1 *Chemicals*

20(*S*)-Ginsenoside Rh2 [20(*S*)-Rh2, purity≥98%] and 20(*R*)-ginsenoside Rh2 [20(*R*)-Rh2, purity≥98%] were purchased from Ambo Institute (Seoul, Korea). Gelatin, sodium nitrite, sodium dodecyl sulfate (SDS), 3-(4,5-dimethylthiazol-2-yl)-2,5-diphenyltetrazolium bromide (MTT), 2′,7′-dichlorofluorescein diacetate (DCFH-DA), and Griess reagent were obtained from Sigma Chemical Co. (St Louis, MO, USA). Dulbecco's modified Eagle's medium (DMEM), fetal bovine serum (FBS), penicillin-streptomycin and trypsin-EDTA were from HyClone Laboratories Inc. (Logan, UT, USA). All other chemicals used were of highest grade commercially available.

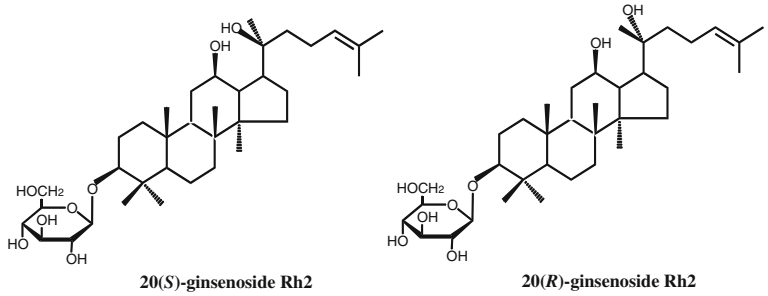

Figure 1. The chemical structures of the two stereoisomers of ginsenoside Rh2 (Rh2), 20(*S*)-ginsenoside Rh2 [20(*S*)-Rh2] and 20(*R*)-ginsenoside Rh2 [20(*R*)-Rh2].

2.2 *Cell culture*

An immortalized human keratinocytes cell line HaCat (ATCC, Manassas, VA, USA) was cultured in DMEM containing 10% heat-inactivated FBS, 100 U/mL penicillin and 100 μg/mL streptomycin in a humidified atmosphere with 5% CO_2 at 37°C. Prior to the treatments, the 1×10^5 HaCat cells were seeded on 24-well plates and cultured overnight, washed twice with 1 mL phosphate-buffered saline (PBS), and replaced with 1 mL FBS-free medium. For confocal microscopic analysis, the 3×10^5 HaCat cells were seeded on 6-well plates.

2.3 *UV-B irradiation*

Ultraviolet lamp (peak, 312 nm; model VL-6M, Vilber Lourmat, Marine, France) was used as a UV-B source. The radiation intensity was monitored using a radiometer (model VLX-3W, Vilber Lourmat) with a sensor (bandwidth, 280 to 320 nm; model CX-312, Vilber Lourmat). The mammalian cells were irradiated with 70 mJ/cm^2 of UV-B for experiments.

2.4 *Detection of intracellular ROS production*

For fluorometric analysis of intracellular ROS, the redox-sensitive fluorescent probe DCFH-DA, which generates the fluorescent 2′,7′-dichlorofluorescein (DCF; $\lambda_{excitation}$ = 485 nm, $\lambda_{emission}$ = 530 nm) upon enzymatic reduction and subsequent oxidation by ROS, was used as previously described (Royall and Ischiropoulos 1993). After incubation with 20(*S*)-Rh2 or 20(*R*)-Rh2 and 10 μM DCFH-DA for 30 min at 37°C, the cells were twice washed with 1 mL FBS-free medium. Then, the cells are replaced with 1 mL FBS-free medium and irradiated with 70 mJ/cm^2 UV-B. The intracellular ROS levels were immediately analysed by Multi-Mode Microplate Reader (Synergy™ Mx, BioTek Instruments, Winooki, VT, USA).

For confocal microscopic analysis, the cells were incubated with 20(*S*)-Rh2 or 20(*R*)-Rh2 and 10 μM DCFH-DA for 30 min at 37°C, irradiated with 70 mJ/cm^2 UV-B, and immediately analysed using Confocal Laser Scanning Microscope (Fluoview-FV300, Olympus, Tokyo, Japan). These assays were repeated at least three times.

2.5 *Determination of nitrite in culture supernatants*

Accumulated nitrite (NO_2^-), generated from cell-released NO, in the culture supernatants was determined using a spectrophotometric assay based on the Griess reaction (Sherman *et al.* 1993). In brief, an equal volume of Griess reagent (1% sulfanilamide-0.1% *N*-1-naphthylethylenediamine dihydrochloride in 2.5% phosphoric acid) was incubated with culture supernatants for 10 min at room temperature, and the absorbance at 550 nm was measured with an enzyme-linked immunosorbent assay (ELISA) reader (Molecular Devices, Sunnyvale, CA, USA). The calibration curve was constructed using known concentrations (0 – 160 μM) of sodium nitrite.

2.6 *Cell viability assay*

To assess the cellular survival of HaCat cells in the presence of 20(*S*)-Rh2 or 20(*R*)-Rh2, the cell viability was determined using MTT assay used to assess metabolic activity (Freshney 1994). The cells were treated with 20(*S*)-Rh2 or 20(*R*)-Rh2 for 30 min. After removing the medium by suction, the cells were incubated with 5 μg/mL MTT solution in medium for 4 h. The cells were then lysed with dimethyl sulfoxide, and the amount of formazan, produced from reduction of MTT by the mitochondria of living cells, was determined by the absorbance at 540 nm.

2.7 *Gelatin zymography*

The gelatinolytic activities of MMP-2 and -1 in culture supernatants were determined by zymographic analysis as previously described (Kleiner and Stetler-Stevenson 1994). The cells were further incubated for 24 h at 37°C, and twice washed with 1 mL PBS. The cells in 1 mL FBS-free medium were incubated with 20(*S*)-Rh2 or 20(*R*)-Rh2 for 30 min and irradiated with 70 mJ/cm^2 UV-B. The culture supernatants, obtained from the irradiated culture incubated for 24 h at 37°C, were fractionated on 10% (w/v) SDS-PAGE gel impregnated with 1 mg/mL gelatin under a non-reducing condition. The proteins in the gel were renatured by shaking with 2.5% Triton X-100 at room temperature for 30 min, which was repeated two times, and incubated in incubation buffer (50 mM Tris buffer, pH 7.8, 5 mM $CaCl_2$, 0.15 M NaCl, 1% Triton X-100) for 24 h. After the gel was stained with a solution of 0.1% Coomassie Brilliant Blue R-250, gelatin-degrading enzymes were convinced as clear zones against a blue background. Identification of MMP-2 and -1 activity bands was in accordance with their molecular weights estimated using molecular mass markers.

2.8 *Western blot analysis*

In order to detect MMP-2 secreted into the culture medium, the culture supernatants, prepared for the zymographic analysis, were used for western blotting analysis. Western blotting was performed using anti-MMP-2 (ALX-210-753, Enzo Life Sciences, Farmingdale, NY, USA) antibody. The culture supernatants were run on 10% polyacrylamide gels and

electrotransferred to PVDF membranes. The membranes were blocked with blocking buffer (2% bovine serum albumin in 1x TBS-Tween 20), probed with primary antibody overnight at 4°C, incubated with secondary antibody (goat anti-rabbit IgG-pAb-HRP-conjugate; ADI-SAB-300, Enzo Life Sciences, Farmingdale, NY, USA) for 1 h at room temperature, and developed with the use of an enhanced West-save up ^{TM} (AbFrontier, Seoul, Korea).

2.9 *Statistical analysis*

The results were represented as mean ± SD. Statistical comparisons between experimental groups were performed using Kruskal-Wallis test, followed by Dunn's *post hoc* test for pairwise individual comparison. A *P*-value less than 0.05 was considered to be statistically significant.

3. Results

3.1 *ROS-scavenging activity under UV-B irradiation*

Since the intracellular ROS level increases under a variety of stresses, especially oxidative stress, it is thought as one of the cellular markers which are closely linked with the stress level inside cells. In the present work, the cultured HaCat cells were treated with varying concentrations of the two Rh2 stereoisomers, 20(*S*)-Rh2 and 20(*R*)-Rh2, prior to 70 mJ/cm^2 UV-B irradiation. As shown in figures 2A and 3A, the UV-B irradiation, in the absence of prior Rh2 treatment, caused the ROS level to significantly increase in HaCat cells, when compared with that in the non-irradiated control cells. 20(*S*)-Rh2 diminished the ROS level, enhanced by the irradiation with 70 mJ/cm^2 UV-B, in a concentration-dependent fashion (figure 2A). At the concentrations of 5, 12 and 30 μM, 20(*S*)-Rh2 made the enhanced ROS level drop to 94.9%, 53.8% and 29.9%, respectively (figure 2A). In contrast with this, 20(*R*)-Rh2, at the same concentrations, was not able to modulate the ROS level enhanced under UV-B irradiation (figure 3A). The ROS-scavenging effect of 20(*S*)-Rh2 but not 20(*R*)-Rh2 was conformed using confocal microscopic analysis (figure 4). Collectively, the two Rh2 stereoisomers act differently in diminishing the ROS level of the HaCat cells under UV-B irradiation, and only the *S*-type stereoisomer of Rh2, 20(*S*)-Rh2, is capable of diminishing the ROS level enhanced under UV-B irradiation.

3.2 *NO-scavenging activity under UV-B irradiation*

Nitric oxide (NO•, NO) is involved in normal physiological processes when produced in minute quantities by

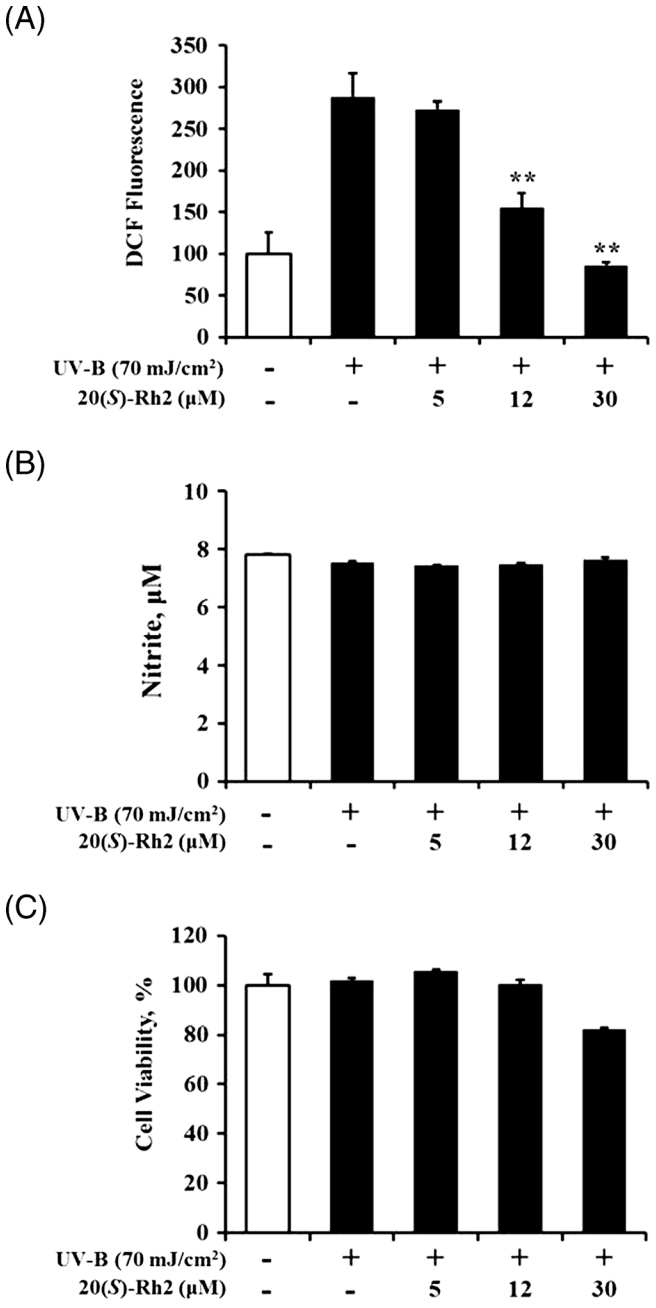

Figure 2. Effects of 20(*S*)-Rh2 on the reactive oxygen species (ROS, **A**) and nitric oxide (NO, **B**) levels, and cellular viability (**C**) in the human HaCat keratinocytes under irradiation with 70 mJ/cm^2 UV-B. In **A**, the ROS level was determined using DCFH-DA in a microplate fluorometer. The ROS level was represented as DCF fluorescence, an arbitrary unit. In **B**, accumulated nitrite, an index of NO, in the culture supernatants was determined by the Griess reaction. In **C**, the viable cell number, represented as the relative percentages, was determined using the MTT assay. Each bar shows the mean ± SD of the three independent experiments repeated in triplicate. **, $P<0.01$ versus the non-treated control (irradiation only).

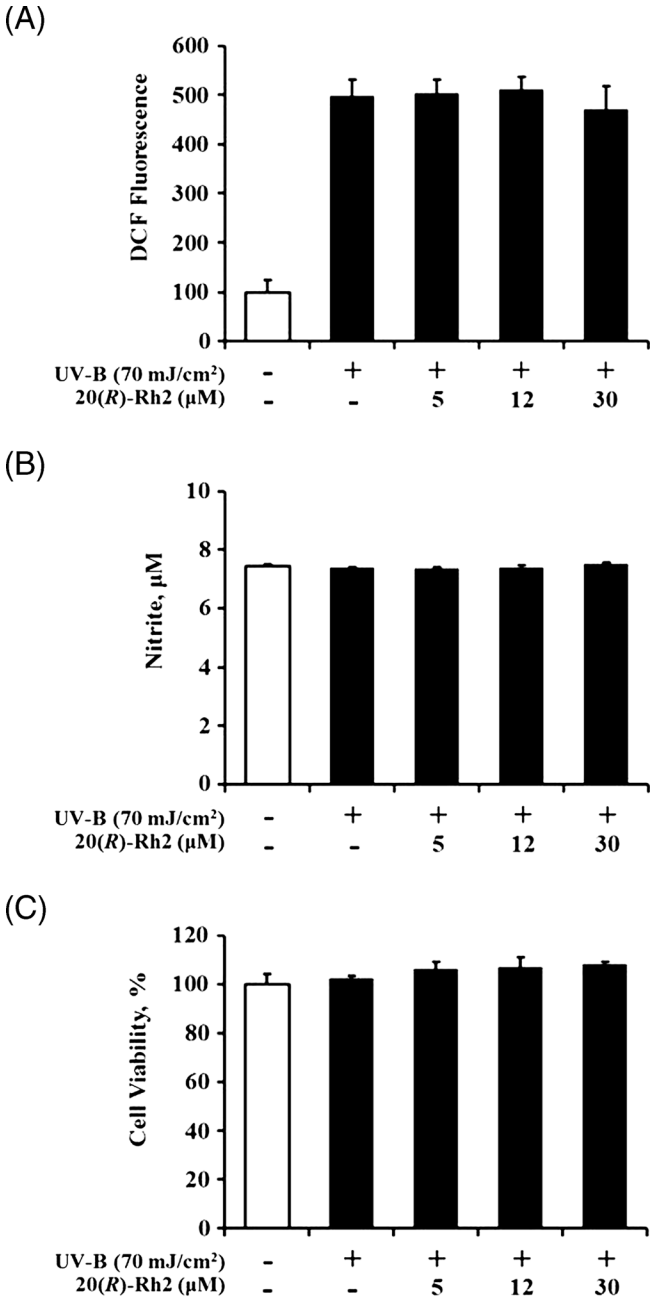

Figure 3. Effects of 20(*R*)-Rh2 on the reactive oxygen species (ROS, **A**) and nitric oxide (NO, **B**) levels, and cellular viability (**C**) in the human HaCat keratinocytes under irradiation with 70 mJ/cm^2 UV-B. In **A**, the ROS level was determined using DCFH-DA in a microplate fluorometer. The ROS level was represented as DCF fluorescence, an arbitrary unit. In **B**, accumulated nitrite, an index of NO, in the culture supernatants was determined by the Griess reaction. In **C**, the viable cell number, represented as the relative percentages, was determined using the MTT assay. Each bar shows the mean ± SD of the three independent experiments repeated in triplicate.

constitutive nitric oxide synthases (cNOSs), while it has pathologic effects when produced in higher quantities by inducible nitric oxide synthase (iNOSs) in the response to various causes. To determine whether NO participates in the response to UV-B irradiation or not, the NO level was measured in the UV-B-irradiated HaCat cells in the absence of 20(*S*)-Rh2 or 20(*R*)-Rh2. As shown in figure 2B and 3B, the NO level in the UV-B irradiated cells appeared to be very similar to that in the non-irradiated cells, and remained unchanged even in the presence of 20(*S*)-Rh2. Similarly, 20(*R*)-Rh2 was unable to modulate the NO level in the HaCat cells under UV-B irradiation (figure 3B). Collectively, NO is not involved in the response to UV-B irradiation, and its level is not modulated by both 20(*S*)-Rh2 and 20(*R*)-Rh2 in the UV-B-irradiated HaCat cells.

3.3 *Cell viability*

To test whether 20(*S*)-Rh2 and 20(*R*)-Rh2, at the concentrations used in this work, exhibit cytotoxicity or not, their effects on the cell viability of HaCat cells were determined using MTT assay. 20(*S*)-Rh2 was unable to significantly modulate the cellular viability of HaCat cells, but 20(*S*)-Rh2 at 30 μM exhibited a tendency of diminishing the cellular viability of HaCat cells (figure 2C). As shown in figure 3C, 20(*R*)-Rh2, at the used concentrations, showed no cytotoxicity on HaCat cells. Taken together, both 20(*S*)-Rh2 and 20(*R*)-Rh2, at the used concentrations, exhibit no significant cytotoxicity on HaCat cells.

3.4 *Matrix metalloproteinases*

Chronic exposure to UV irradiation disrupts normal architecture of the skin, which causes skin photoaging. UV irradiation induces expression of certain members of the MMP family, such as MMP-1, -2 and -9, which are capable of degrading collagen and other extracellular matrix proteins that comprise the dermal connective tissue (Quan *et al.* 2009). Scavenging and quenching of ROS by antioxidants and inhibition of MMP activity and expression are thought to be efficient strategies to prevent and reduce skin photoaging. When the gelatinolytic activities of MMP-2 and -1 were detected in the UV-B irradiated HaCat cells using gelatin zymography, the gelatinolytic activity of MMP-2 was significantly enhanced but that of MMP-1 remained uninduced (figure 5). 20(*S*)-Rh2, at the concentrations of 5, 12 and 30 μM, was capable of diminishing the UV-B-induced MMP-2 activity in a concentration-dependent manner, and couldn't modulate the MMP-1 activity at the level uninduced by UV-B (figure 5A). 20(*R*)-Rh2, at the same concentrations, could diminish the UV-B-induced MMP-2 activity in a

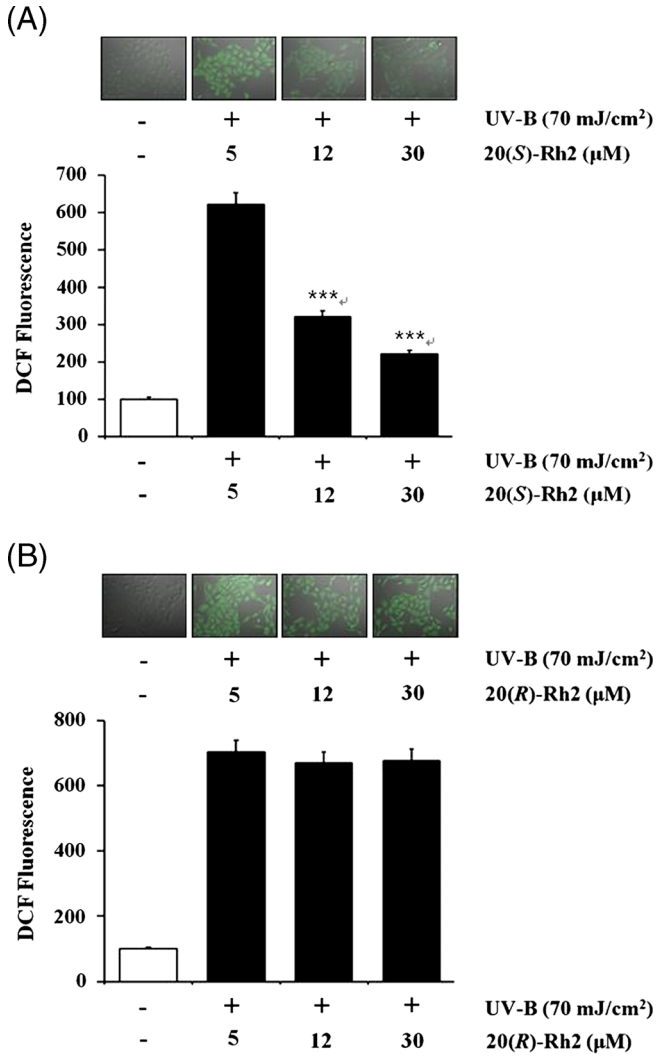

Figure 4. Effects of 20(*S*)-Rh2 (**A**) and 20(*R*)-Rh2 (**B**) on the reactive oxygen species (ROS) levels in the human HaCat keratinocytes under irradiation with 70 mJ/cm^2 UV-B. The ROS levels were determined using DCFH-DA followed by confocal laser scanning microscopy. Representatives of the three independent experiments are shown. In the lower panels of both **A** and **B**, the ROS-associated fluorescent signals, expressed as percentage control, were quantified using Adobe Photoshop software (Adobe Systems, Mountain View, CA). ***, $P<0.001$ versus the non-treated control (UV-B irradiation only).

concentration-dependent manner and maintained the MMP-1 activity at the uninduced level.

Modulation of MMP-2 activity by 20(*S*)-Rh2 and 20(*R*)-Rh2 in the UV-B irradiated HaCat cells was examined at protein level using western blotting analysis. As shown in figure 6, the MMP-2 protein level significantly increased in the culture supernatants of HaCat cells under the irradiation with 70 mJ/cm^2 UV-B. 20(*S*)-Rh2 diminished the UV-B-induced MMP-2 protein level in HaCat cells (figure 6A). In a similar way, 20(*R*)-Rh2 was able to diminish the UV-B-induced MMP-2 protein level in HaCat cells in a concentration-dependent manner (figure 6B). Taken together, 20(*S*)-PPD and 20(*R*)-PPD down-regulate the UV-B-induced MMP-2 of HaCat cells at protein level.

4. Discussion

UV-A and UV-B are major causes of photoaging, which is characterized by wrinkles, laxity, coarseness, and mottled pigmentation, and photocancers (Jenkins 2002; Rittié and Fisher 2002). UV-B acts primarily on the epidermal basal cell layer of the skin, leading the initiation of a photooxidation reaction which impairs the antioxidant status of the skin and increases cellular level of ROS (Ikehata and Ono 2011). Keratinocytes, the major cell population in the basal layer, are the primary targets of UV-B. Enhanced ROS levels are accompanied by the activation of ROS-sensitive signaling pathways. UV-B results in apoptotic cell death of HaCat cells following enhancements in ROS and superoxide radical levels after the irradiation (Paz *et al.* 2008). However, NO level remains unchanged in HaCat cells under UV-B irradiation, suggesting that NO is not involved in the apoptotic cell death caused by UV-B (Paz *et al.* 2008). Similarly to these findings, UV-B irradiation significantly increased the ROS level in HaCat cells, which was detected using both fluorometric and confocal microscopic analyses. Prior treatments of the two Rh2 stereoisomers exhibited different ROS-scavenging activities. In keratinocyte cells, only the *S*-type stereoisomer appeared to possess an ROS-scavenging activity. The two Rh2 stereoisomers were unable to modulate the NO level of HaCat cells unaffected under UV-B irradiation. Together with the previous findings, the cellular damages caused by UV-B irradiation seem to be mediated by the intracellular ROS level not by the NO level. Mechanism(s) responsible for the stereospecific ROS-scavenging effect of Rh2 remain to be solved. One possibility is that 20(*S*)-Rh2 inhibits the enzymatic activities responsible for the generation of ROS in a stereospecific manner. Another possibility is that 20(*S*)-Rh2 directly reacts with ROS species, which is hardly understood when considering the stereospecific effect of 20(*S*)-Rh2, a relatively small molecule. A third possibility is that 20(*S*)-Rh2 activates or induces antioxidant proteins which abolish the ROS species in a stereospecific manner.

UV radiation, including UV-B, activates and induces one or more MMPs and then cause damages to the skin, resulting in skin photoaging. For example, UV-A activates MMP-1 through the involvement of oxidative stress, under which there is excessive generation of ROS and/or depletion of antioxidant functions in the skin cells including keratinocytes and fibroblasts (Pygmalion *et al.* 2010). 20(*S*)-Rh2, which is capable of scavenging intracellular

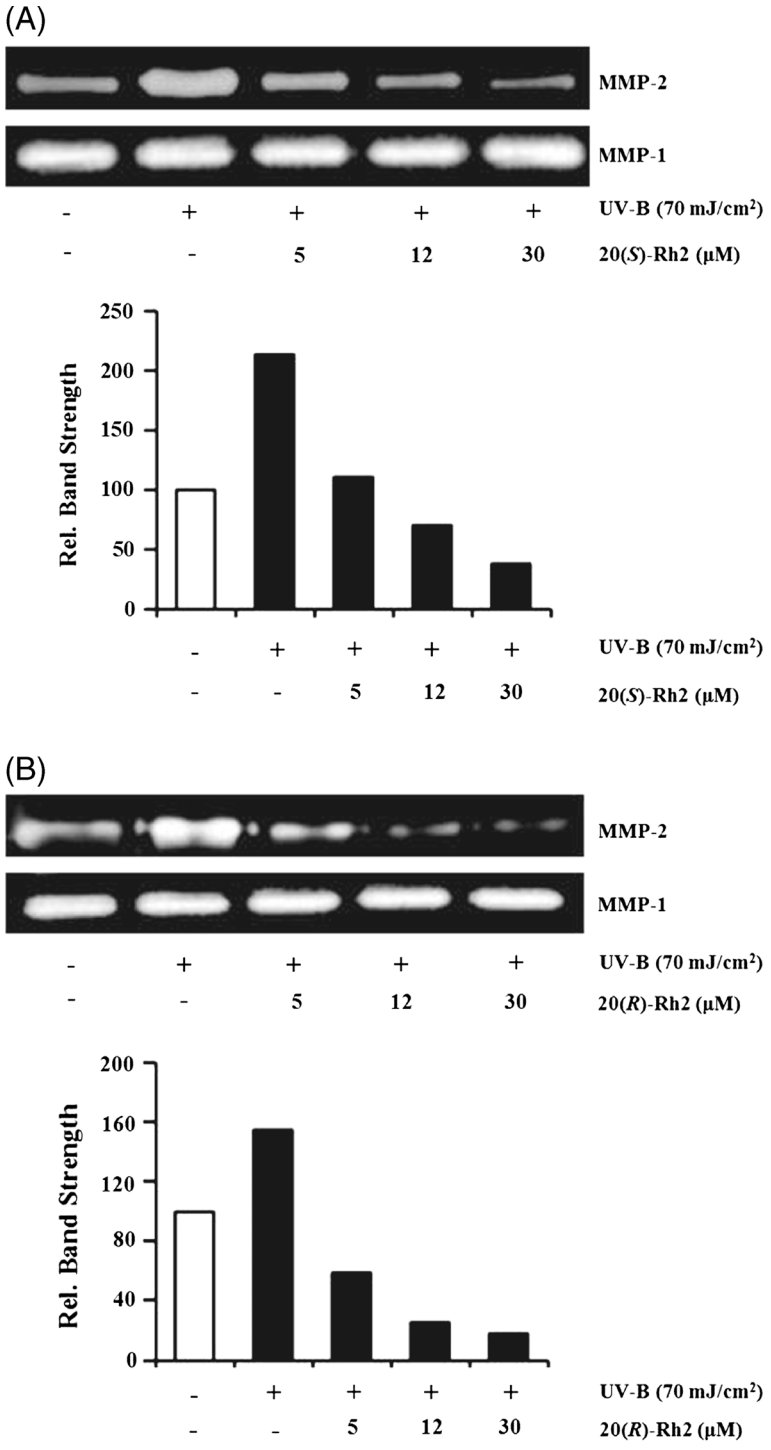

Figure 5. Effects of 20(*S*)-Rh2 (**A**) and 20(*R*)-Rh2 (**B**) on matrix metalloproteinase-2 and -1 (MMP-2 and -1) activities in the human HaCat keratinocytes under irradiation with 70 mJ/cm^2 UV-B. The gelatinolytic activities of MMP-2 and -1 in the culture supernatants were detected using gelatin zymography. Representatives of the three independent experiments are shown. In the lower panels of both **A** and **B**, relative band strength (relative density normalized to MMP-1) was determined with densitometry using the ImageJ software which can be downloaded from the NIH website.

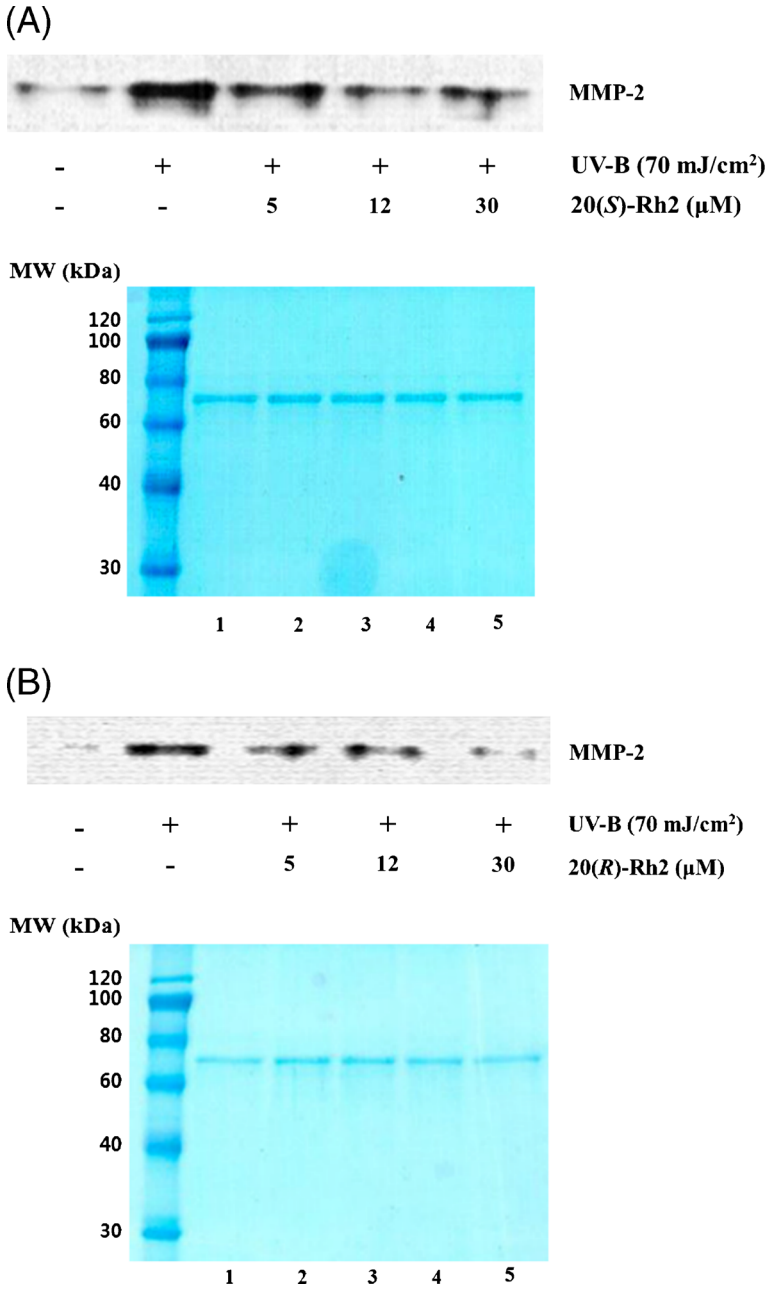

Figure 6. Effects of 20(*S*)-Rh2 (**A**) and 20(*R*)-Rh2 (**B**) on matrix metalloproteinase-2 (MMP-2) levels in the human HaCat keratinocytes under irradiation with 70 mJ/cm^2 UV-B. The MMP-2 levels in the culture supernatants were determined using western analysis with anti-MMP-2 antibodies. Representatives of the three independent experiments are shown. In the lower panels of both **A** and **B**, the equal loading of the culture supernatants was shown by the use of Coomassie Blue staining of the identical gels.

ROS, exhibit a down-regulating effect on UV-B-induced MMP-2 activity and expression, implying its skin anti-photoaging activity. 20(*R*)-Rh2 was also found to suppress UV-B-induced MMP-2 activity and expression, although its suppressive activity seems to be weaker than that of 20(*S*)-Rh2. These results suggest that both 20(*S*)-Rh2 and 20(*R*)-Rh2 have skin anti-photoaging activities through down-regulation of UV-B-induced MMP-2 activity and expression but in different mechanisms. 20(*S*)-Rh2 suppresses the UV-B-induced MMP-2 in a ROS-dependent fashion, whereas 20(*R*)-Rh2 suppresses it in a ROS-independent fashion. An interesting result, obtained in this work, is that MMP-2 but

not MMP-1 and MMP-9 is induced in HaCat cells by UV-B irradiation and the enhanced MMP-2 level is down-regulated by the Rh2 stereoisomers. Similar findings on the involvement of MMP-2 in the response to UV-B irradiation have been identified. Increased production of MMP-2 but not MMP-9 was found in human corneal fibroblasts in response to UV-B, especially in the acute phase after the irradiation (Kożák *et al*. 2003). A daily use cream containing a photostable combination of UV-B and UV-A absorbers reduces the MMP-2 mRNA enhanced in the buttock skin biopsies of healthy volunteers exposed to solar simulated radiation (Seité *et al.* 2000). Sargachromenol, isolated from *Sargassum horneri*, a brown alga growing on the coastal sea of Korea and Japan, plays a down-regulating role in UV-B-induced MMP-2 mRNA level in skin dermal fibroblasts (Kim *et al.* 2012). Although pyruvate don't inhibit UV-B-induced enhancement of intracellular ROS in HaCat cells, it is able to enhance the survival rate of the UV-B-irradiated cells through the suppression of UV-B-induced mRNA expression of inflammatory mediators (Aoki-Yoshida *et al.* 2013). This indirectly supports that the cellular damages caused by UV-B irradiation can be recovered in a ROS-independent fashion.

Until recently, several purified components and extracts have been identified to possess MMP inhibitory activities of skin cells in diverse mechanisms. For example, a hydroethanolic extract of *Butea monosperma* (Lam.) Taub. flowers, a common Indian plant widely used for inflammatory diseases, is able to diminish the secretion of MMP-1, -2, -9 and -10 in addition to pro-inflammatory cytokines and prostaglandin E2 production in UV-B-treated normal human epidermis keratinocytes (Krolikiewicz-Renimel *et al.* 2013). Although retinoids are one of well-known anti-aging ingredients, their application can cause photo-sensitive responses such as skin irritation, which prevents their daytime usage (Park *et al.* 2013).

In conclusion, the skin anti-photoaging activities of the two stereoisomers of ginsenoside Rh2, 20(*S*)-Rh2 and 20(*R*)-Rh2, were individually examined in the HaCat cells exposed to UV-B radiation. 20(*S*)-Rh2, but not 20(*R*)-Rh2, suppresses the UV-B-induced ROS level. However, both 20(*S*)-Rh2 and 20(*R*)-Rh2 diminish the UV-B-induced MMP-2 activity and expression. 20(*S*)-Rh2 and 20(*R*)-Rh2 have skin anti-photoaging properties through the suppression of MMP-2 possibly via ROS-dependent and –independent fashions, respectively. Ginsenoside Rh2 can be used as a natural resource for manufacturing anti-aging cosmetics.

Acknowledgements

This study was supported by a grant of the Korea Healthcare Technology R&D Project, Ministry of Health & Welfare, Republic of Korea (Grant No. : A103017). This study was also supported by 2014 Research Grant from Kangwon National University (No. 120140161).

References

Aitken GR, Henderson JR, Chang SC, McNeil CJ and Birch-Machin MA 2007 Direct monitoring of UV-induced free radical generation in HaCaT keratinocytes. *Clin. Exp. Dermatol.* **32** 722–727

Aoki-Yoshida A, Aoki R and Takayama Y 2013 Protective effect of pyruvate against UVB-induced damage in HaCaT human keratinocytes. *J. Biosci. Bioeng.* **115** 442–448

Bae EA, Han MJ, Kim EJ and Kim DH 2004 Transformation of ginseng saponins to ginsenoside Rh2 by acids and human intestinal bacteria and biological activities of their transformants. *Arch. Pharm. Res.* **27** 61–67

Baek NI, Kim DS, Lee YH, Park JD, Lee CB and Kim SI 1996 Ginsenoside Rh4, a genuine dammarane glycoside from Korean red ginseng. *Planta Med.* **62** 86–87

Barresi C, Stremnitzer C, Mlitz V, Kezic S, Kammeyer A, Ghannadan M, Posa-Markaryan K, Selden C, *et al*. 2011 Increased sensitivity of histidinemic mice to UVB radiation suggests a crucial role of endogenous urocanic acid in photoprotection. *J. Invest. Dermatol.* **131** 188–194

Birch-Machin MA and Swalwell H 2010 How mitochondria record the effects of UV exposure and oxidative stress using human skin as a model tissue. *Mutagenesis* **25** 101–107

Curran S and Murray GI 1999 Matrix metalloproteinases in tumour invasion and metastasis. *J. Pathol.* **189** 300–308

Freshney RI 1994 *Culture of animal cells: a manual of basic technique* 4th edition (New York: Wiley-Liss Press)

Hwang JT, Kim SH, Lee MS, Kim SH, Yang HJ, Kim MJ, Kim HS, Ha J, *et al*. 2007 Anti-obesity effects of ginsenoside Rh2 are associated with the activation of AMPK signaling pathway in 3T3-L1 adipocyte. *Biochem. Biophys. Res. Commun.* **364** 1002–1008

Ichihashi M, Ueda M, Budiyanto A, Bito T, Oka M, Fukunaga M, Tsuru K and Horikawa T 2003 UV-induced skin damage. *Toxicology* **189** 21–39

Ikehata H and Ono T 2011 The mechanisms of UV mutagenesis. *J. Radiat. Res.* **52** 115–125

Jenkins G 2002 Molecular mechanisms of skin ageing. *Mech. Ageing. Develop.* **123** 801–810

Kähäri VM and Saarialho-Kere U 1997 Matrix metalloproteinases in skin. *Exp. Dermatol.* **6** 199–213

Kim JA, Ahn BN, Kong CS and Kim SK 2012 Protective effect of chromene isolated from *Sargassum horneri* against UV-A-induced damage in skin dermal fibroblasts. *Exp. Dermatol.* **21** 630–631

Kleiner DE and Stetler-Stevenson WG 1994 Quantitative zymography: detection of picogram quantities of gelatinases. *Anal. Biochem.* **218** 325–329

Kożák I, Klisenbauer D and Juhás T 2003 UV-B induced production of MMP-2 and MMP-9 in human corneal cells. *Physiol. Res.* **52** 229–234

Krolikiewicz-Renimel I, Michel T, Destandau E, Reddy M, André P, Elfakir C and Pichon C 2013 Protective effect of a *Butea*

monosperma (Lam.) Taub. flowers extract against skin inflammation: Antioxidant, anti-inflammatory and matrix metalloproteinases inhibitory activities. *J. Ethnopharmacol.* **148** 537–543

Lee YM, Kim YK, Kim KH, Park SJ, Kim SJ and Chung JH 2009 A novel role for the TRPV1 channel in UV-induced matrix metalloproteinase (MMP)-1 expression in HaCaT cells. *J. Cell. Physiol.* **219** 766–775

Liu J, Shimizu K, Yu H, Zhang C, Jin F and Kondo R 2010 Stereospecificity of hydroxyl group at C-20 in antiproliferative action of ginsenoside Rh2 on prostate cancer cells. *Fitoterapia* **81** 902–905

Liu J, Shiono J, Shimizu K, Yu H, Zhang C, Jin F and Kondo R 2009 20(R)-ginsenoside Rh2, not 20(S), is a selective osteoclastgenesis inhibitor without any cytotoxicity. *Bioorg. Med. Chem. Lett.* **19** 3320–3323

Park EK, Choo MK, Kim EJ, Han MJ and Kim DH 2003 Antiallergic activity of ginsenoside Rh2. *Biol. Pharm. Bull.* **26** 1581–1584

Park NH, Park JS, Kang YG, Bae JH, Lee HK, Yeom MH, Cho JC and Na YJ 2013 Soybean extract showed modulation of retinoic acid-related gene expression of skin and photoprotective effects in keratinocytes. *Int. J. Cosmet. Sci.* **35** 136–142

Paz ML, González Maglio DH, Weill FS, Bustamante J and Leoni J 2008 Mitochondrial dysfunction and cellular stress progression after ultraviolet B irradiation in human keratinocytes. *Photodermatol. Photoimmunol. Photomed.* **24** 115–122

Pygmalion MJ, Ruiz L, Popovic E, Gizard J, Portes P, Marat X, Lucet-Levannier K, Muller B, *et al*. 2010 Skin cell protection against UVA by sideroxyl, a new antioxidant complementary to sunscreens. *Free Radic. Biol. Med.* **49** 1629–1637

Quan T, Qin Z, Xia W, Shao Y, Voorhees JJ and Fisher GJ 2009 Matrix-degrading metalloproteinases in photoaging. *J. Invest. Dermatol. Symp. Proc.* **14** 20–24

Rittié L and Fisher GJ 2002 UV-light-induced signal cascades and skin aging. *Ageing Res. Rev.* **1** 705–720

Royall JA and Ischiropoulos H 1993 Evaluation of 2',7'-dichlorofluorescin and dihydrorhodamine 123 as fluorescent probes for intracellular H_2O_2 in cultured endothelial cells. *Arch. Biochem. Biophys.* **302** 348–355

Seité S, Colige A, Piquemal-Vivenot P, Montastier C, Fourtanier A, Lapière C and Nusgens B 2000 A full-UV spectrum absorbing daily use cream protects human skin against biological changes occurring in photoaging. *Photodermatol. Photoimmunol. Photomed.* **16** 147–155

Sherman MP, Aeberhard EE, Wong VZ, Griscavage JM and Ignarro LJ 1993 Pyrrolidine dithiocarbamate inhibits induction of nitric oxide synthase activity in rat alveolar macrophages. *Biochem. Biophys. Res. Commun.* **191** 1301–1308

Trinh HT, Han SJ, Kim SW, Lee YC and Kim DH 2007 Bifidus fermentation increases hypolipidemic and hypoglycemic effects of red ginseng. *J. Microbiol. Biotechnol.* **17** 1127–1133

Werb Z 1997 ECM and cell surface proteolysis: regulating cellular ecology. *Cell* **91** 439–442

Zhang C, Yu H and Hou J 2011 Effects of 20(S)-ginsenoside Rh2 and 20(R)-ginsenoside Rh2 on proliferation and apoptosis of human lung adenocarcinoma A549 cells. *Zhongguo Zhong Yao Za Zhi* **36** 1670–1674

Zhang J, Zhou F, Niu F, Lu M, Wu X, Sun J and Wang G 2012 Stereoselective regulations of P-glycoprotein by ginsenoside Rh2 epimers and the potential mechanisms from the view of pharmacokinetics. *PLoS One* **7** e35768

MS received 07 February 2014; accepted 23 June 2014

Corresponding editor: B Jagadeeshwar Rao